Transaction B: Mechanical Engineering
Vol. 16, No. 1, pp. 92–100

Research Note

Prediction of Stratified Charge Divided Chamber Engine Performance

M. Tiourad[1] and A. Mozafari[1,*]

Abstract. *Certain stratified charge divided chamber engines have a very small pre-chamber, equipped with a spark plug and a main chamber connected to the pre-chamber through nozzles. A theoretical model is presented in this research to predict ignition delay and initiation of combustion in the pre-chamber. It considers flame progress in the pre-chamber up to the point where the flame penetrates the main chamber through the connecting nozzles. Step by step calculations then continue in the main chamber and the mass fraction burned and the energy release rate are calculated. The process continues to the point where all the fuel is burned. At each step, due to a one degree rotation of the crank shaft, there is a change in the cylinder volume, due to the movement of the piston and, also, a change in the mole fraction burned, due to the burning of a fraction of the mixture. Considering heat transfer from the cylinder contents to its surrounding area, some important operating parameters, such as indicated power, indicated thermal efficiency, indicated specific fuel consumption, indicated mean effective pressure and volumetric efficiency, are predicted. Stepwise calculations also provide in-cylinder pressure-volume and pressure-crank angle diagrams, as well as the in-cylinder contents temperature variation with the crank position and concentration of species existing in the combustion products. Predicted values obtained by the present model are compared with corresponding experimental values available in the literature to evaluate the accuracy of the model. The comparison shows reasonable agreement between theoretical and measured values.*

Keywords: *Divided chamber; Stratified charge; Modelling; Engine performance.*

INTRODUCTION

Since the introduction of internal combustion engines, spark ignition engines have always benefitted from a reliable location and time of ignition or initiation of combustion by using a spark plug in a relatively rich mixture of air and fuel, whereas compression ignition engines have had advantages, regarding lean burning, higher efficiencies and less pollutant emission by auto ignition of a lean and well compressed mixture of air and fuel.

It is possible to ignite a small fraction of fuel by employing a spark in a very small chamber, called a pre-chamber or an auxiliary chamber, to ensure reliability in the location and time of initiation of combustion. As the combustion progresses in the pre-chamber, the flame front penetrates the main chamber through nozzles connecting the two chambers (see Figure 1). A very lean mixture of air and fuel in the main chamber then can easily be ignited by these penetrating flame streams, resulting in a lean burn combustion with higher efficiency and less pollution. The new engine is a divided chamber stratified charge engine, which carries the advantages of both SI and CI engines.

Pre-chamber volume and shape, as well as the number of orifices and their directions, affect the velocity, pressure and kinetic turbulence energy of the pre-chamber contents [1]. Also, engine thermal efficiency, specific fuel consumption and exhaust emissions of CO, HC and NO_x are affected by the engine compression ratio and the fuel air equivalence ratio [2].

Experimental research shows that engine heat transfer, main cylinder pressure and pollutants of CO and HC in the exhaust gas depend on the piston head shape [3] and that the fuel spray angle and direction of the orifices connecting the two chambers have influences on engine fuel consumption, power output and exhaust emissions [4].

The effects of fuel injection and ignition times on

1. *Department of Mechanical Engineering, Sharif University of Technology, P.O. Box 11155-9567, Tehran, Iran.*
*. *Corresponding author. E-mail: mozafari@sina.sharif.edu*

Received 6 February 2007; received in revised form 4 December 2007; accepted 7 April 2008

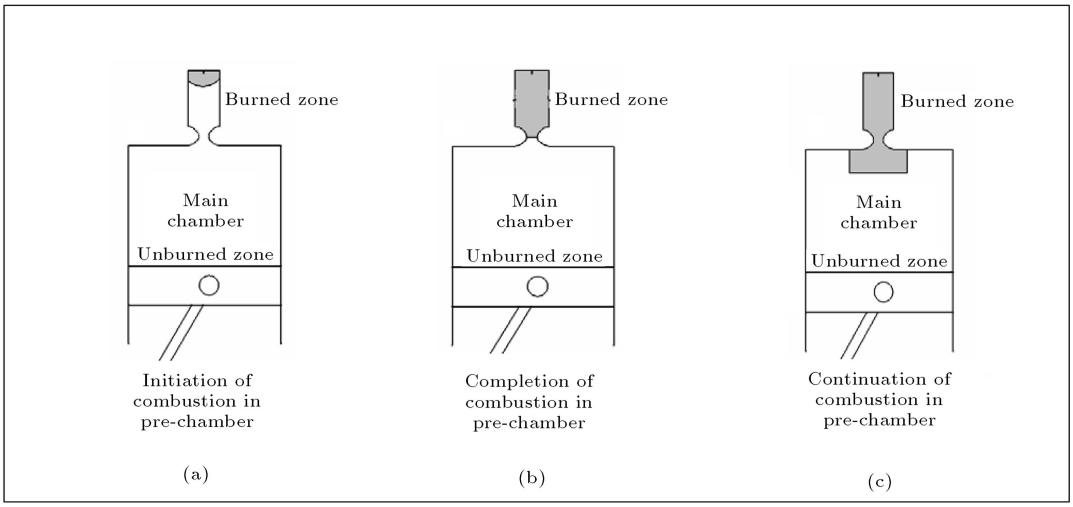

Figure 1. Schematic view of combustion process in divided chamber engine.

engine performance, and the predicted variation with the crank angle of cylinder pressure and mass fractions of H_2O and NO in the exhaust gas, were investigated by Zheng et al. [5] using the FIRE code with a $k-\varepsilon$ turbulence model. Other research shows the effects of the fuel air equivalence ratio on flame behavior in a cylindrical pre-chamber using ethylene fuel in a wide range of air fuel ratios [6].

In the present work, the combustion delay time and initiation of combustion in the pre-chamber, as well as the combustion progress in both chambers, are studied. The effects of compression ratio, fuel air equivalence ratio and engine speed on the mass fraction burned, in-cylinder pressure, indicated thermal efficiency and specific fuel consumption are predicted for iso-octane and methane fuels.

THEORETICAL MODEL, GOVERNING EQUATIONS AND ASSUMPTIONS

In the present model, various processes taking place in the pre-chamber and main chamber have been considered in detail. The model can be applied to any fuel with the chemical formula $C_xH_yO_z$ in a liquid or vapor phase. The calculations start from the end of the induction stroke and the compression process is from this point to the predetermined crank angle at which the spark occurs in the pre-chamber. There is a continuation of compression for a specific period of time, known as delay time, which is needed for initiation of combustion at the pre-chamber. It is assumed that compression of the mixture of air and fuel continues during this period. The extent of delay time can be estimated as the time needed for burning a finite volume of fuel air mixture [7] or the burning of a special representative eddy [8,9], whilst some consider it as a finite number of crank angle degrees [10,11] and others ignore the effects of delay altogether [12,13]. The present model assigns the delay period as the time needed for burning 0.1 percent of the chamber content, as recommended by Benson et al. [7].

The combustion process then starts in the pre-chamber and continues to the point at which the flame occupies all the pre-chamber volume. The flame then penetrates to the main chamber through the connecting orifices, resulting in an initiation of combustion in the main chamber. The combustion process continues to the point at which all the fuel is reacted. The expansion process is considered from the end of combustion (where flame propagation terminates) up to the bottom dead center.

The theoretical model is concerned with the step-wise calculation of the thermodynamic state for the combustion chamber contents. The physical properties of individual constituents and the mixture of gases during the cycle are calculated as follows.

The most suitable relation in order to give very accurate values of the molar specific heat capacity of ideal gases at a wide range of temperatures, from 298 K to 6000 K, is provided by Mozafari [14] in the form of:

$$C_P(T) = F_1(T)^3 + F_2(T)^2 + F_3(T) + F_4 + F_5(T)^{-1} + F_6(T)^{-2} + F_7(T)^{-3} + F_8(T)^{-4} + F_9(T)^{-5} + F_{10}(T)^{-6}. \quad (1)$$

Having the coefficients of F_i for any constituent facilitates the calculation of molar values of enthalpy, entropy, internal energy and Gibbs function and, consequently, equilibrium constants for the reactions involved.

For a mixture of n different ideal gases, the values of the above mentioned properties are obtained by

using relation $\sum_{i=1}^{n} x_i A_i$, where x_i is mole fraction and A_i is the related property of substance i in the mixture.

For viscosity $\mu(T)$ and thermal conductivity $\lambda(T)$ of an ideal gas at temperature T, a relation in the form of:

$$\mu(T) = f_1(T)^{2.5} + f_2(T)^2 + f_3(T)^{1.5} + f_4(T) + f_5(T)^{0.5} + f_6 + f_7(T)^{-0.5}, \quad (2)$$

and:

$$\lambda(T) = f_5'(T)^{2.5} + f_2'(T)^2 + f_3'(T)^{1.5} + f_4'(T) + f_5'(T)^{0.5} + f_6' + f_7'(T)^{-0.5}, \quad (3)$$

which are presented by Mozafari [14], are employed. Values of the coefficients, F_i, f_i and f_i' in Equations 1-3 for the substances involved are given by Mozafari [14].

For a mixture of n different ideal gases, an equation in the form of:

$$\lambda_m = \sum_{i=1}^{n} \frac{y_i \lambda_i}{\sum_{j=1}^{n} y_j A_{ij}}, \quad (4)$$

due to Wassiljewa [15], for the thermal conductivity of the mixture, and an equation in the form of:

$$\mu_m = \sum_{i=1}^{n} \frac{x_i \mu_i}{\sum_{j=1}^{n} x_j \varphi_{ij}}, \quad (5)$$

due to Chapman-Enskog [15], for the dynamic viscosity of the mixture, are used. A_{ij} and φ_{ij} are expressed as:

$$A_{ij} = k \frac{\left[1 + (\lambda_{tri}/\lambda_{trj})^{1/2} (M_i/M_j)^{1/4}\right]^2}{[8(1 + M_i/M_j)]^{1/2}}, \quad (6)$$

and:

$$\varphi_{ij} = \frac{\left[1 + (\mu_i/\mu_j)^{1/2} (M_j/M_i)^{1/4}\right]^2}{[8\,(1 + M_i/M_j)]^{1/2}}, \quad (7)$$

using the Mason & Saxena modification and the Wilke approximation, respectively [15].

At every step during the cycle, there is a small change of volume for the main chamber, due to a rotation of the crank shaft and a corresponding movement of the piston. The relation, $P\Delta V$, represents the related work. There is also heat transfer from the cylinder contents to its surrounding surfaces for each step, which is determined by using the Annand correlation [16,17].

$$\delta q = a \left(\frac{k_{\text{mix}}}{B}\right) \text{Re}^b (T_g - T_w) + c(T_g^4 - T_w^4). \quad (8)$$

The fuel is assumed to have the chemical formula $C_x H_y O_z$, where x, y and z may be set to quantities that suit the fuel. The combustion products are considered to be carbon dioxide, carbon monoxide, water vapor, hydrogen, oxygen, nitrogen and unburned fuel. Three more reactions are taken into account in the combustion chamber, which are:

$$CO + \frac{1}{2} O_2 \leftrightarrow CO_2, \quad (9)$$

$$CO + H_2O \leftrightarrow CO_2 + H_2, \quad (10)$$

$$xCO_2 + \frac{y}{2} H_2 \leftrightarrow C_x H_y O_z + (x - 0.5z) O_2. \quad (11)$$

Four equations of mass balance for carbon, oxygen, hydrogen and nitrogen, plus three more equations provided by the equilibrium constants of the above reactions, are used to calculate the mole fractions of the products.

Energy released during the combustion process at each step, due to the burning of a small volume of the mixture, is determined by assuming a turbulent flame propagation rate, $U_T = k_t U_L$, where k_t is the turbulent flame factor representing the total effects of turbulence and U_L is the laminar flame speed, expressed by Kuehl [18], in the form of:

$$U_L = \frac{7784\,(P_0/P)^x}{[10000/T_b + 900/T_U]^{4.938}}. \quad (12)$$

Mass interaction between the pre-chamber and the main chamber through the orifice areas connecting the two chambers, are considered by employing the orifice flow equation [19] in the form of:

$$Q = C_0 A_0 \sqrt{\frac{2(P_1 - P_2)}{\rho\left[1 - \left(\frac{D_0}{D}\right)^4\right]}}. \quad (13)$$

The direction of flow (which regularly changes during a cycle) depends on instantaneous pressures of the chambers, dictated by movement of piston and combustion process in the chambers (see Figure 2). Ignoring the change of potential energies of the control volume and the kinetic energies of the initial and final states of the contents, the energy conservation equation for a constant volume pre-chamber may be written as:

$$Q_{\text{C.V.}} + m_i \left(h_i + \frac{V_i^2}{2}\right) = m_e \left(h_e + \frac{V_e^2}{2}\right) + (m_2 u_2 - m_1 u_1), \quad (14)$$

where for the main chamber, due to the movement of the piston and the resulting change of volume, the

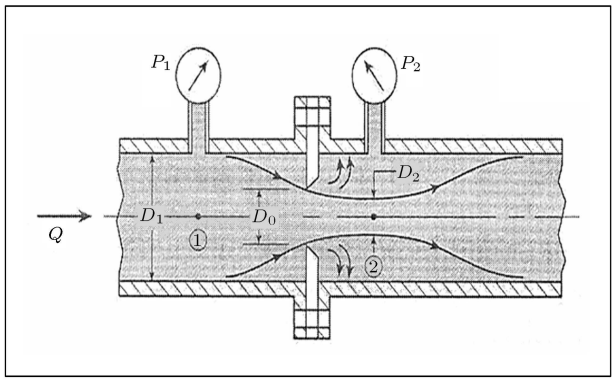

Figure 2. Schematic view of flow through orifice.

equation would be:

$$Q_{\text{C.V.}} + m_i \left(h_i + \frac{V_i^2}{2} \right) = m_e \left(h_e + \frac{V_e^2}{2} \right) + (m_2 u_2 - m_1 u_1) + W_{\text{C.V.}}. \quad (15)$$

One should notice that, depending on the direction of flow through the orifice, for some of the steps during the cycle, either m_i or m_e, for the pre-chamber, is zero and, at any time, the quantity of m_i for the pre-chamber is equal to the quantity of m_e for the main chamber and vice-versa. Also, the conservation of mass equation for both chambers relates the quantities of mass at the initial and final states to the mass crossing the chambers through the orifices.

The principles of energy and mass conservation are applied to each step during the cycle in order to find the final state of the step, since the properties at the initial state are known. The properties at the final state could all be depending on one unknown parameter (chosen to be temperature), thus, the right value of the temperature is the one that satisfies the energy balance equation within a prescribed tolerance.

VERIFICATION OF PRESENT MODEL

Pre-Chamber

To estimate the validity and accuracy of the present model, the performance of a stratified charge divided chamber engine, using CH_4 as fuel, is predicted. The results for the pre-chamber are compared with the experimental values for the same chamber, using natural gas, published by Roubaud et al. [20]. Engine specifications and experimental running conditions (expressed by Rounaud et al. and presented in Table 1) are employed in the model to predict ignition delay, initiation of combustion and flame propagation in the pre-chamber. The results are shown in Figures 3 to 7.

Note that the pre-chamber volume is only 3% of the total cylinder volume and calculations at every step involve mass transaction between this tiny volume

Table 1. Divided chamber engine specifications and experimental running conditions by Roubaud [20].

Manufacturer	Liebherr
Nozzle orifices	4 orifices of 2 mm
Type	G 926 TI
Number of cylinders	6
Bore	122 mm
Stroke	142 mm
Conrod Length	228 mm
Total Swept Volume	9096 L
Pre-chamber Volume	mm^3 4540
Volumetric Compression Ratio	12.0 or 13.3
Turbocharger	KKK K27 3371 OLAKB
Crank Shaft Rotation Speed	1500 ± 5 rpm
Ignition System	Fairbank Morse IQ 250
Number of Valves	2
Rated Brake Mean Effective Pressure	150 ± 1.3 kW
Intake Air Pressure	960 ± 5 mbar
Intake Air Temperature	25 ± 2° C
Intake Air Relative Humidity	50 ± 0.5 %
Exhaust Gas Pressure After Turbocharger	1050 ± 3 mbar
Spark Plugs	Bosch Super F & W6DC

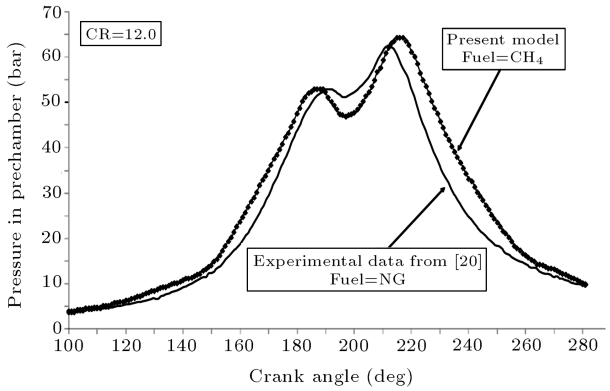

Figure 3. Variation with crank angle of predicted and experimental values of pressure in pre-chamber.

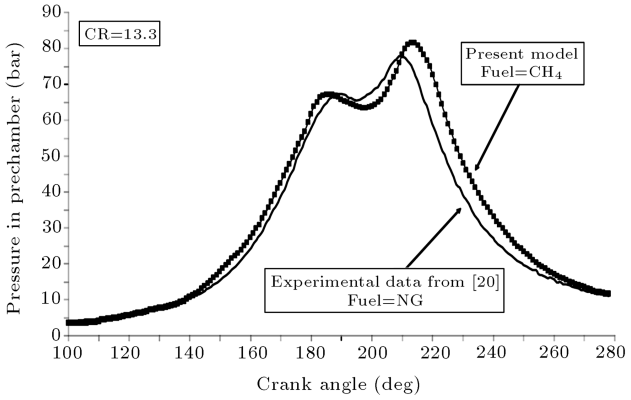

Figure 4. Variation with crank angle of predicted and experimental values of pressure in pre-chamber.

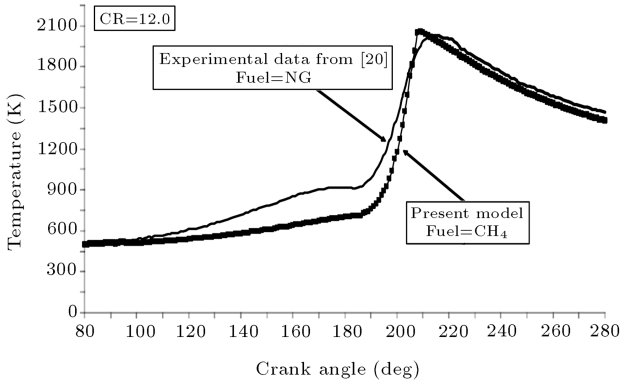

Figure 5. Variation with crank angle of present predicted and predicted values of temperature, based on measured pressure values [20] in pre-chamber.

and the main chamber. Also, due to the fact that the properties of the final states of the two chambers are related, the predicted results for the pre-chamber are highly sensitive and the assumptions used must be in very good agreement with reality, otherwise, the predicted behavior of pressure and mass variations in the pre-chamber will considerably differ from those measured experimentally.

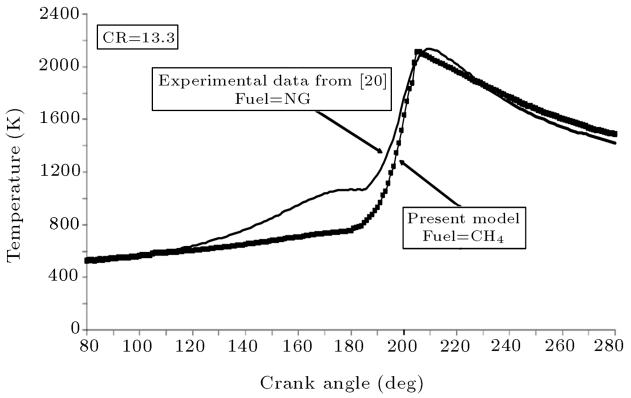

Figure 6. Variation with crank angle of present predicted and predicted values of temperature, based on measured pressure values [20] in pre-chamber.

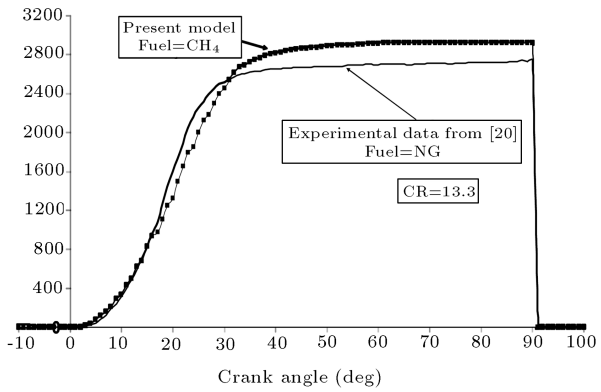

Figure 7. Variation with crank angle of predicted and experimental values of heat release.

As seen in Figures 3 and 4, the predicted trends of the variation and behavior of pressure in the pre-chamber are compatible with measured values, having an average deviation of about 5%. Also, an average deviation of 7% between the present predicted and the predicted values of the temperature, based on measured pressure values [20], indicates the reasonable accuracy of the model.

The compatibility of the experimental values of heat release for natural gas, with predicted values for methane, is shown in Figure 7.

Main Chamber

To ensure the accuracy of the calculations for the main chamber, experimental data from a normal 4 cylinder spark ignition engine were compared with the predicted values obtained by the model for the same engine. Since the engine was not equipped with a pre-chamber, the volume of the pre-chamber in the theoretical model was set to zero, thus, the calculations due to the pre-chamber, were ignored.

In such cases, the combustion in the main chamber starts from the point of the spark plug, the flame

propagates spherically in all directions and the rate of heat release is calculated accordingly.

Table 2 shows the single chamber engine specifications and experimental running conditions used for this comparison.

The experimental and predicted results for the main chamber are shown in Figures 8 and 9.

As seen from these figures, the predicted values of the indicated power and the indicated specific fuel consumption obtained for C_8H_{18} are compatible with corresponding experimental values obtained by measured brake and friction powers. A maximum deviation of 7% for indicated power and of 1.5% for thermal efficiency and fuel consumption shows quite acceptable agreement between measured and predicted values.

THEORETICAL RESULTS AND DISCUSSION

The performance of a stratified charge divided chamber engine is predicted and the results for the mass fraction burned, the instantaneous pressure, the indicated thermal efficiency and the indicated specific fuel consumption are shown in Figures 10 to 14.

According to the results, a higher compression ratio resulted in shorter combustion duration, indicating faster flame propagation (see Figure 10). It also resulted in a higher pressure and temperature for the cycle (see Figures 11 and 12). Increasing the engine speed provided a higher power output, a higher thermal efficiency and lower specific fuel consumption. These results indicate that the behavior of stratified charge divided chamber engines follows that of normal single cylinder engines, but they are capable of running on leaner mixtures and at higher compression ratios. Comparison of the results show that stratified charge engines have a lower ignition delay time (due to a richer mixture in the pre-chamber) and a faster burning rate

Table 2. Single chamber engine specifications and experimental running conditions. [21]

Cylinder Swept Volume	1323 cc
Number of Cylinders	4
Bore	71 mm
Stroke	83.6 mm
Compression Ratio	9.7
Intake Air Pressure	100 kPa
Intake Air Temperature	300K

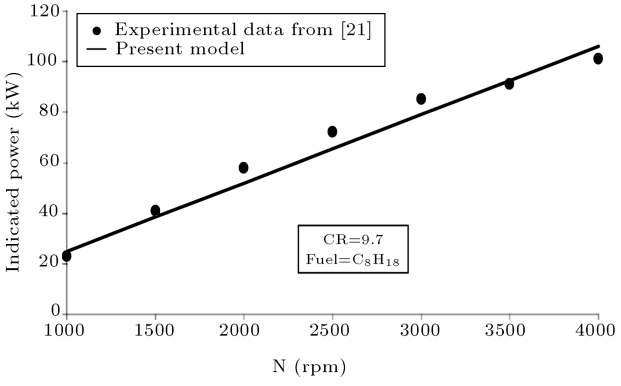

Figure 8. Variation of indicated power with engine speed.

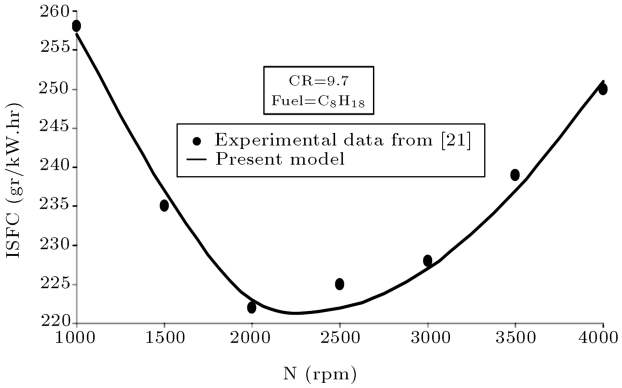

Figure 9. Variation of indicated specific fuel consumption with engine speed.

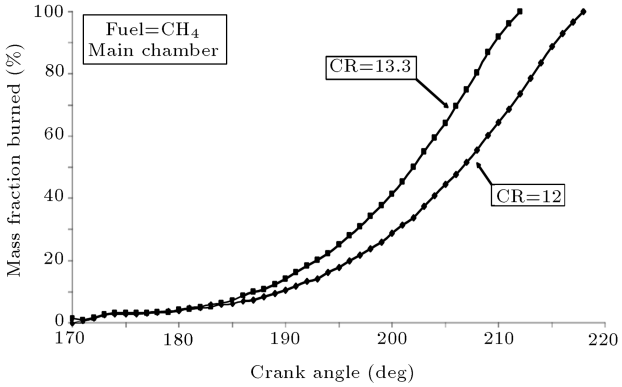

Figure 10. Variation with crank angle of predicted mass fraction burned.

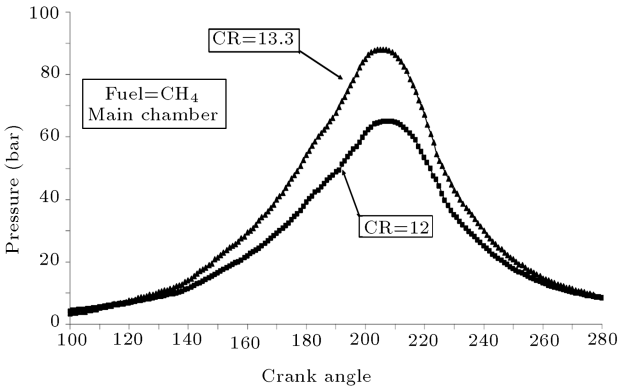

Figure 11. Variation with crank angle of predicted pressure in main chamber.

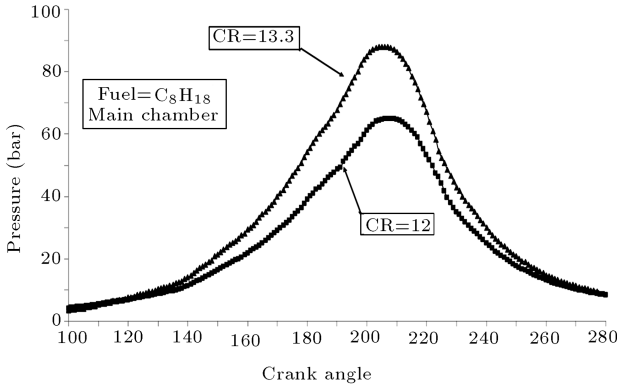

Figure 12. Variation with crank angle of predicted pressure in main chamber.

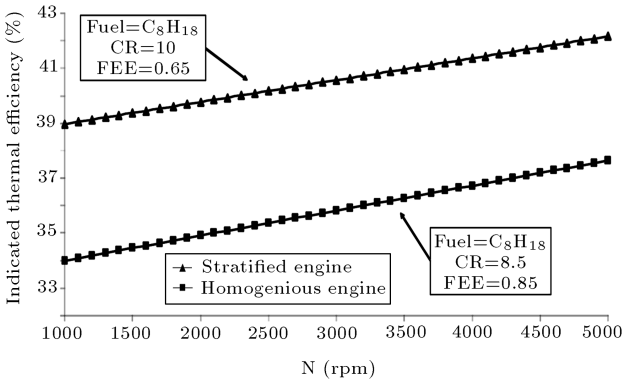

Figure 13. Variation of indicated thermal efficiency with engine speed.

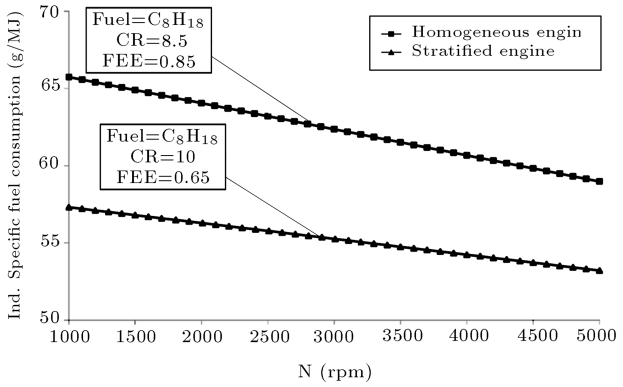

Figure 14. Variation of indicated specific fuel consumption with engine speed.

(dictated by a higher compression ratio), however, the values depend on the running conditions.

Initiation of combustion in a very small pre-chamber is assured by a relatively rich mixture. However, the main combustion takes place at the main chamber, which contains a very lean mixture, providing higher thermal efficiency and lower fuel consumption. Also, this lean mixture allows the engine to run at a higher compression ratio, which, normally, would have caused knock in a normal engine.

To show the advantages of divided chamber engines, regarding fuel consumption and thermal efficiency, the results are compared with corresponding values predicted for a normal combustion chamber engine, with similar specifications and optimum running conditions (see Figures 13 and 14). These results indicate that divided chamber engines have higher thermal efficiencies or lower fuel consumptions of up to 15%, at compression ratios and fuel air equivalence ratios typically suitable for these engines. Considering the huge number of engines running on daily bases and the quantity of fuel burned, this reduction in fuel consumption is highly important, especially for countries such as Iran, which currently imports vast quantities of fuel. The equilibrium concentrations of pollutants CO and HC in the exhaust gas of a divided chamber engine are predicted to be less than those of a normal single cylinder engine, apparently because of the leaner burning associated with a divided chamber engine. This is compatible with expectations and the level of reduction depends on running conditions, mainly air fuel ratio and compression ratio. Also, for a leaner mixture, fewer quantities of unburned HC are caused by quenching distance and crevices.

The divided chamber engines have a lower combustion temperature, with cleaner combustion and less concentrations of NO_x in the resulting exhaust gas.

Since the aim of the present research was to develop a theoretical model to consider the major phenomena in the pre-chamber and main chamber of a divided chamber engine, including their effects on each other, the level of concentration of NO_x had no effect on the related output data and, thus, it was excluded from the combustion products. Of course, one should notice that the formation of NO_x is highly important, regarding pollution, and the next step for the authors is to continue research on the pollution issue of divided chamber engines and to complete the present model with the inclusion of NO_x in the exhaust gas.

CONCLUSION

A theoretical model is developed to predict the performance of stratified charge engines, using any fuel with chemical formula $C_xH_yO_z$ in a liquid or vapor phase by considering the compression, combustion and expansion process in the pre-chamber and main chamber.

Heat transfer from in-cylinder contents to the surrounding surfaces, as well as work due to the movement of pistons in the main chamber, is considered. Mass interaction between the pre-chamber and main chamber through the orifice areas connecting the two chambers is calculated. Comparison of the predicted

results with published experimental values indicates that:

1. The model predicts the instantaneous pressures and temperatures of the contents in the pre-chamber and main chamber of the stratified charge engines with acceptable accuracy;
2. Heat release and mass fraction burned, obtained by the model, is in very good agreement with published measured values;
3. Higher compression ratios will provide a higher power output, higher thermal efficiency, lower fuel consumption, a faster burning rate and shorter combustion duration;
4. Stratified charge engines have a lower ignition delay time, indicating a quicker initiation of combustion, due to a much richer mixture in their pre-chambers;
5. Stratified charge engines consume up to 15% less fuel, compared to normal homogenous charge engines;
6. Stratified charge engines provide a lower combustion temperature, due to their leaner mixtures.

NOMENCLATURE

A	area
A_i	related property of substance i
B	cylinder diameter
c	coefficient of flow
CI	compression ignition
C_p	specific heat at constant pressure
CR	compression ratio
f_i	coefficient of equation for viscosity
f_i'	coefficient of equation for thermal conductivity
F_i	coefficient of equation for C_p
h	enthalpy
k_m	thermal conductivity of the mixture
k_t	turbulent flam factor
m	mass
M_i	molecular weight of substance i
NG	natural gas
P	pressure
q	heat transfer rate
Q	heat transfer
Re	Reynolds number
SI	spark ignition
T	temperature
u	internal energy
U	flame speed
V	velocity
V	volume
W	work
X_i	mole fraction of substance i

Greek Symbols

λ_i	thermal conductivity of substance i
λ_m	thermal conductivity of mixture
μ_i	dynamic viscosity of substance i
μ_m	dynamic viscosity of mixture
ρ	density
φ	fuel air equivalence ratio
θ	crank angle

Subscript

b	burned
C.V.	control volume
g	gas
e	exit
i	inlet
i	substance i
L	laminar
mix	mixture
0	reference point
T	turbulent
u	unburned
w	wall

REFERENCES

1. Kowalewicz, A., *Combustion Systems of High-Speed Piston I.C. Engines, Warszawa* (1984).
2. Stone, R., *Introduction to Internal Combustion Engines*, MacMillan (1992).
3. Roethlisberger, R.P. and Favrat, D. "Comparison between direct and indirect (pre-chamber) spark ignition in the case of a cogeneration natural gas engine. Part I: Engine geometrical parameters", *Applied Thermal Engineering*, **22**, pp. 1217-1229 (2002).
4. Roethlisberger, R.P. and Favrat, D. "Investigation of the pre-chamber geometrical configuration of a natural gas spark ignition engine for cogeneration. Part II. Experimentation", *International Journal of Thermal Sciences*, **42**, pp. 239-253 (2003).
5. Zheng, Q.P., Zhang, H.M. and Zhang, D.F. "A computational study of combustion in compression ignition natural gas engine with separated chamber", *Fuel*, **84**, pp. 1515-1523 (2005).
6. Cattolica, R.J., Barr, P.K. and Mansour, N.N. "Propagation of a premixed flame in a divided-chamber combustor", *Combustion and Flame*, **77**, pp. 101-121 (1989).

7. Benson, R.S., Annand, W.J.D. and Baruah, P.C. "A simulation model including intake and exhaust systems for a single cylinder four-stroke cycle spark-ignition engine", *Int. J. Mech. Sci. Pergamon Press*, **17**, pp. 97-124 (1975).
8. Hires, S.D., Tabaczynski, R.J. and Novak, J.M. "The prediction of ignition delay and combustion intervals for a homogenous charge, spark-ignition engines", *SAE Trans.*, **87**, p. 1053 (1978).
9. Tabaczynski, R.J., Trinker, F.H. and Shanon, B.A.S. "Further refinement and validation of a turbulent flame propagation model for spark-ignition engines", *Combustion and Flames*, **39**, p. 111 (1980).
10. Heywood, J.B., Haggins, J.M., Watts, P.A. and Tabaczynski, R.J. "Development and use of a cycle simulation to predict S-I engine efficiency and NO_x emissions", *Society of Automotive Engineers Inc.*, **790291** (Feb. 1979).
11. Blumberg, P. and Kummer, J.T. "Prediction of NO formation in spark ignition engines", *An Analysis of Methods of Control*, Gordon and Breach, Science Publishers Limited, Combustion Science and Technology, **4**, p. 73 (1971).
12. Lucas, G.G. and James, E.H. "A computer simulation of a spark-ignition engine", Society of Automotive Engineers, International Automative Engineering, Detroit, Mich., **730053** (Jan. 1973).
13. Patterson, D.J. and Van Wylen, G. "A digital computer simulation for spark-ignition engine cycles", *Progress in Technology*, **7**, NY, SAE Inc. (1964).
14. Mozafari, A. "Predictions and measurement of spark ignition engine characteristics using ammonia and other fuels", Ph.D. Thesis, University of London (1988).
15. Reid, R.C., Prausnitz, J.M. and Sherwood, T.K., *The Properties of Gases and Liquids*, 3rd Ed., McGraw Hill (1977).
16. Annand, W.J.D. "Heat transfer in the cylinders of reciprocating internal combustion engines", *Inst. Mech. Engineers Proc.*, **177**(36), pp. 973-96 (1966).
17. Heywood, J.B., *Internal Combustion Engine Fundamentals*, McGraw Hill (1998).
18. Benson, R.S. *Internal Combustion Engine*, Pergamon Press (1983).
19. Esposito, A. *Fluid Mechanics with Applications*, Prentice Hall (1998).
20. Roubaud, A. and Favrat, D. "Improving performances of a lean burn cogeneration biogas engine equipped with combustion pre-chambers", *Fuel*, **84**, pp. 2001-2007 (2005).
21. Neyestani, J. "Experimental investigation of air temperature and flow velocity distribution inside engine compartment", M.Sc. Thesis, Sharif University of Technology (Jan. 2006).